Int. J. Heat Mass Transfer. Vol. 8, pp. 589–607. Pergamon Press 1965. Printed in Great Britain

TEMPERATURE PROFILE IN THE ENTRANCE REGION OF AN ANNULAR PASSAGE CONSIDERING THE EFFECTS OF TURBULENT CONVECTION AND RADIATION

LESTER D. NICHOLS†

Lewis Research Center, National Aeronautics and Space Administration, Cleveland, Ohio

(*Received* 25 *October* 1963 *and in revised form* 17 *September* 1964)

Abstract—The influence of the absorption of radiation on the temperature profile and heat transfer to an absorbing medium flowing in an annulus has been examined analytically. In the analysis, a turbulent, non-gray gas stream with variable density and temperature-dependent absorption coefficients are considered. The results of the analysis are compared with those of an experiment performed with steam flowing at Reynolds numbers near 20 000 at pressures of 1·0 and 3·22 atm in an annulus with a radius ratio of 0·2. The analytical result agrees with the experimental result that for an inner wall temperature of 2000°R and a pressure of 3·22 atm the absorption of radiation increases the temperature slightly (about 7 per cent). This result is also in qualitative agreement with results of Viskanta's analysis for a stagnant fluid in a plane parallel geometry.

NOMENCLATURE

A_n, expansion coefficients defined in equation (34);

$a(T, P)$, ratio of line width to line spacing;

$a_i(T, P)$, dimensionless absorption coefficients;

B_n, expansion coefficients defined in equation (55);

B^*_ω, B^*_λ, B^*_i, Planck function for wave number ω, wavelength λ, or the i^{th} band;

b^*, line width;

C, constant;

C_n, D_n, expansion coefficients defined in equation (57);

c^*_p, specific heat at constant pressure;

e, normalized eddy diffusivity;

$F^{(1)}_i$, $F^{(2)}_i$, $F^{(s)}_i$, absorption integrals defined in equations (C1), (C2), and (C3), respectively;

$\mathbf{F}^*_r$, radiation flux vector;

$f^{(1)}_i$, $f^{(2)}_i$, absorption integrals in equations (B3) and (B4);

G, dimensionless net radiation absorption function;

$G^{(1)}$, $G^{(2)}$, dimensionless net radiation absorption function defined in equations (B1) and (B2);

$G^{(1)}_i$, $G^{(2)}_i$, absorption integrals defined in equations (C5) and (C4), respectively;

$g^{(2)}_i$, absorption integral defined in equation (B5);

$H^*_{w,\omega}(T^*)$, intensity at a surface for a given wave number;

$H^{(1)}_i(T^*)$, $H^{(2)}_i(T^*)$, dimensionless intensity at a given band on surface one and surface two for temperature T^*;

h_i, dimensionless ratio of Planck function, $B_i(T^*)/B_{\max}(T_2)$;

I_0, I_1, Bessel functions of zero and first order of imaginary argument;

J_1, J_2, intensity impinging on surface one and surface two;

† Much of this research was performed at Case Institute of Technology with the guidance and helpful advice of Professor Jerzy R. Moszynski and presented as a Ph.D. thesis.

K_i^*, mass absorption coefficient for i^{th} band;
k^*, thermal conductivity;
L, length of path for radiation;
M, radiation interaction parameter,

$$\frac{R_2^* a_{max}(T_2^*) B_{max}^*(T_2^*)}{\rho_2^* T_2^* c_p^* \ln (T_1^*/T_2^*) (\epsilon_h)_{max}};$$

$\dot{m}^*$, mass flow rate;
P^*, pressure;
Q^*, heat transferred;
Q_{abs}, Q_{na}, non-dimensional heat transferred to absorbing gas and non-absorbing gas respectively;
R_n, n^{th} characteristic function defined in equation (33);
R_1^*, R_2^*, radius of inner and outer cylinder, respectively;
r, dimensionless radial co-ordinate, r^*/R_2^*;
r^*, radial co-ordinate;
s^*, s_1^*, s_2^*, element of path length;
s, s_1, s_2, dimensionless path length s^*/R_2^*, S_1^*/R_2^*, S_2^*/R_2^*;
T^*, temperature of gas;
T_1^*, T_2^*, temperatures of inner and outer cylinder, respectively;
u, dimensionless axial velocity;
u^*, axial velocity;
u_{max}^*, maximum value of axial velocity;
v^*, radial velocity component;
x, dimensionless axial co-ordinate, x^*/R_2^*;
x^*, axial co-ordinate;
x_{cr}^*, critical value of axial velocity;
z, reduced axial co-ordinate defined in equation (20);
$a_i^*(T^*)$, absorption coefficient for i^{th} band;
β_i, dimensionless ratio of absorption coefficients, $a_i(T^*)/a_{max}(T_2^*)$;
δ^*, line spacing;
ϵ_h, eddy diffusivity for heat transfer;
ϵ_1, ϵ_2, emissivity of inner and outer cylinder;
η, variable in equation (13);
Θ, dimensionless function of temperature,

$$\frac{\ln T^* - \ln T_2^*}{\ln T_1^* - \ln T_2^*};$$

Θ_{ent}, entrance temperature;
Θ_{fd}, fully developed temperature profile;
Θ_j, dimensionless temperatures in equation (28);
θ_1, θ_2, θ_1^*, θ_2^*, angles shown in Fig. 6;
κ_ω^*, mass absorption coefficient for wave number ω;
λ_n, n^{th} characteristic value of equation (21);
ξ, dummy variable of integration;
ρ, radius ratio of inner cylinder, R_1^*/R_2^*;
ρ^*, density;
ρ_2^*, density at outer wall;
$\tau_i^{(1)}$, $\tau_i^{(2)}$, optical path length for i^{th} band defined in equation (A6);
τ_ω, optical path length for wavelength, λ;
$\Phi_n(z)$, expansion coefficients defined in equation (44);
$\chi_n(z)$, expansion coefficient defined in equation (48);
Ω_s, solid angle;
ω, wave number, $1/\lambda$;
$\Delta\omega_i$, band widths for i^{th} band.

Superscripts

1, inner surface;
2, outer surface;
*, dimensional quantity.

INTRODUCTION

THE INTERACTION of radiant energy with an absorbing medium has been of engineering interest for quite some time. Recently, the interaction of radiant energy with moving absorbing media, thereby adding another mode

of energy transfer, has become of interest [1–4]. In contrast to most previous analyses of this phenomenon, the present study considers the absorbing medium to be a non-gray gas (that is, having absorption properties that are dependent on wavelength) with absorption properties that depend on temperature. Further, this absorbing medium is considered under conditions of fully developed turbulent flow.

Consider the steady flow of a gaseous absorbing medium in an annular passage with a fully developed turbulent velocity profile. At some point the temperature of the inner cylinder is suddenly increased, while the temperature of the outer cylinder remains unchanged. The subsequent development of the temperature profile and the heat transfer to the gas is the subject of this study. This development takes place in a region called the thermal entrance region. In this region the fluid is assumed to be a perfect gas subject to the following conditions: no heat sources, negligible body forces, constant specific heat, and negligible viscous dissipation. The temperature profile and the heat transfer will be calculated not only for an absorbing gas but also for a non-absorbing gas; in fact, the solution for the absorbing gas is obtained by perturbing the solution to the problem for the non-absorbing gas. This method can be used quite extensively, because the effects of turbulent diffusion will be quite large compared with those due to radiation absorption, except under conditions of extremely high temperatures and pressures. For the case of a non-absorbing gas, the thermal entrance problem will be solved by an extension of the techniques used in the Graetz problem in order to take into account a variable fluid density.

In order to predict the temperature and heat transfer, the turbulent convection as well as the radiation absorption must be determined. The method of describing the turbulence is that wherein an eddy diffusivity for heat transfer is introduced [5–7]. This quantity must be determined experimentally for the pertinent flow conditions. For the present analysis, the eddy diffusivity is determined from measurements of the temperature profile in air [8], and this value is used to calculate the temperature for the steam.

The method of computing the absorption properties of steam is the statistical method described in reference [9]. Herein the absorption is assumed to take place in discrete bands. The dependence of the absorption on temperature and pressure is determined from experimental results [9, 10]. The particular bands to be considered are determined from spectroscopic measurements.

ANALYSIS

Derivation of equations

Consider the thermal entrance length problem for turbulent flow in an annulus. The solution to this problem involves considering the equations of mass, energy, and momentum as well as an equation of state for the fluid. In general, these equations must be considered simultaneously. However, because of their complex nature, certain simplifying assumptions will be made herein.

For the thermal entrance length problem where the velocity profile is fully developed on entering the heating section, there will still be a velocity adjustment in the thermal entrance region to account for the heating and consequent density change. However, for turbulent flow at a region somewhat downstream of the entrance to the heating section, it can be shown experimentally that the velocity can be separated into a product of a function of the axial position and a function of radius as follows:

$$u^* = u^*_{\max}(x^*) \cdot u(r^*) \tag{1}$$

These functions will be determined experimentally for the conditions of interest. An estimate of the length of the region wherein this assumption is not valid must be determined; in this case the determination was experimental.

With the axial velocity profile specified, it is not necessary to consider the momentum equation. The energy equation including radial turbulent diffusion and radiation absorption, but neglecting axial diffusion, may be written as

$$\rho^* c_p^* \left(v^* \frac{\partial T^*}{\partial r^*} + u^* \frac{\partial T^*}{\partial x^*} \right) - \frac{1}{r^*} \frac{\partial}{\partial r^*} \left[r^* (k^* + \rho^* c_p^* \epsilon_h) \frac{\partial T^*}{\partial r^*} \right] = - \operatorname{div} \mathbf{F}_r^* \tag{2}$$

and the continuity equation may be written as

$$\frac{\partial}{\partial r^*}(r^*\rho^* v^*) + \frac{\partial}{\partial x^*}(r^*\rho^* u^*) = 0 \qquad (3)$$

Except in the term involving the radial velocity, temperature is the dependent variable in the energy equation. It will be shown that even in the thermal entrance length, there is a region wherein it is possible to neglect the radial velocity term in the energy equation; i.e.

$$\rho^* v^* \frac{\partial T^*}{\partial r^*} \ll \rho^* u^* \frac{\partial T^*}{\partial x^*}$$

so that the temperature will remain as the only dependent variable. Intuitively, it may be expected that very close to the entrance region the radial temperature gradient would be very large, such that the inequality is not valid. This is indeed the case. Consequently, a determination of the distance x^*_{cr}, it is necessary first to solve the continuity equation for v^*:

$$\rho^* v^* = -\frac{1}{r^*}\int_{R_1^*}^{r^*} \frac{\partial}{\partial x^*}(u^*_{\max}\rho^*)\, u(r^*)\, r^*\, dr^* \qquad (4)$$

Also, an additional requirement must be satisfied, namely, the mass flow rate in the annulus $\dot{m}^*$ must be a constant, where $\dot{m}^*$ is defined as

$$\dot{m}^* = 2\pi\, u^*_{\max}(x^*)\, \rho^*_2 \int_{R_1^*}^{R_2^*} u(r^*)\, \frac{T^*_2}{T^*(x^*, r^*)}\, r^*\, dr^* \qquad (5)$$

where the density variation is specified in terms of the temperature variation. Now $u^*_{\max}$ may be expressed in terms of its value at the entrance to the heated section $u^*_{\max,\,0}$ as

$$u^*_{\max}(x^*) = u^*_{\max,\,0}\, \frac{\int_{R_1^*}^{R_2^*} u(r^*)\, r^*\, dr^*}{\int_{R_1^*}^{R_2^*} u(r^*)\, [T^*_2/T^*(x^*, r^*)]\, r^*\, dr^*} \qquad (6)$$

Hence, $\rho^* v^*$ can be estimated once T^* and u^* are known as functions of r^* and x^*. From experimentally measured temperature and velocities $\rho^* v^*$ can be calculated and x^*_{cr} can be evaluated, so that the region for which the term involving the radial velocity can be neglected may be considered known.

Now, equation (2) may be reduced to read:

$$u^*_{\max}\, u(r^*)\, \rho^* c_p^* \frac{\partial T^*}{\partial x^*} - \frac{1}{r^*}\frac{\partial}{\partial r^*}\left[r^*(k^* + \rho^* c_p^* \epsilon_h)\frac{\partial T^*}{\partial r^*}\right] = -\operatorname{div} \mathbf{F}^*_r. \qquad (7)$$

Equation (7) has two more functions that must be known in order to determine T: ϵ_h and $\operatorname{div} \mathbf{F}^*_r$. The first of these, ϵ_h, will be determined experimentally and thus is known for purposes of analysis at this point. In reference 8 a comparison of this eddy diffusivity with semi-empirical values is made. The second, $\operatorname{div} \mathbf{F}^*_r$, represents the net radiation absorption of the fluid. This term may be evaluated in terms of a radiant energy balance at a control volume as [8, 11–13]:

$$-\operatorname{div} \mathbf{F}^*_r = \int_0^\infty \left\{ \kappa^*_\omega \rho^* \frac{1}{\pi} \int_{\Omega_s = 4\pi} \left[H^*_{w,\,\omega}(T^*) \exp\left[-\tau_\omega(0, s^*)\right] + \int_0^{s^*} B^*_\omega(T^{*\prime}) \exp\left[-\tau_\omega(s^{*\prime}, s^*)\right] \kappa^{*\prime}_\omega \rho^{*\prime}\, ds^{*\prime} \right] d\Omega_s - 4\kappa^*_\omega \rho^* B^*_\omega(T^*) \right\} d\omega \qquad (8)$$

where $H^*_{w,\,\omega}(T^*)$ is the intensity of radiant energy at a surface and τ_ω is the optical path length defined along the physical line of sight as

$$\tau_\omega(s^{*\prime}, s^*) = \int_{s^{*\prime}}^{s^*} \kappa^{*\prime}_\omega \rho^{*\prime}\, ds^{*\prime} \qquad (9)$$

The terms on the right-hand side of equation (8) represent the absorption of radiation from the walls, absorption of radiation from the gas, and emission from the element, respectively. It is immediately evident that the energy balance at a point is influenced by the temperature of the rest of the medium including the boundaries. If it is required that $\operatorname{div} \mathbf{F}^*_r = 0$ when the temperature of the medium is uniform and equal to the temperature of the boundaries, equation (7) may be written as

$$u^*\rho^*c_p^*\frac{\partial T^*}{\partial x^*} - \frac{1}{r^*}\frac{\partial}{\partial r^*}\left[r^*(k^* + \rho^*c_p^*\epsilon_h)\frac{\partial T^*}{\partial r^*}\right]$$

$$= \int_0^\infty \kappa_\omega^*\rho^*\left\{[H_{w,\omega}^*(T_1^*) - H_{w,\omega}^*(T^*)]\int_{\Omega s_1}\frac{1}{\pi}\right.$$

$$\exp[-\tau_\omega(0, s^*)]\,d\Omega_{s_1} - [H_{w,\omega}^*(T^*)$$

$$- H_{w,\omega}^*(T_2^*)]\int_{\Omega s_2}\frac{1}{\pi}\exp[-\tau_\omega(0, s^*)]\,d\Omega_{s_2}$$

$$+\frac{1}{\pi}\int_{\Omega_s=4\pi}\int_0^{s^*}\kappa_\omega^{*'}\rho^{*'}[B_\omega^*(T^{*'}) - B_\omega^*(T^*)]$$

$$\left.\exp[-\tau_\omega(s^{*'}, s^*)]\,ds^{*'}\,d\Omega_s\right\}d\omega \qquad (10)$$

On the right-hand side of this equation are the terms representing the influence of radiation: the first is the net radiation between the inner cylinder and the element under consideration, the second is the net radiation between the outer wall and the element, and the third is the net radiation between the remainder of the fluid volume and the element.

This equation includes consideration of a non-gray gas, temperature dependent absorption properties, and gas to gas radiation as well as turbulent convection–conduction in the thermal entrance region of an annular passage. However, the equation is extremely complicated and further simplication is necessary before it can be solved.

Evaluation of absorption coefficient. The first simplification involves the manner in which the spectral dependence of the absorption coefficient is handled. Usually, the assumption is made that the gas absorbs only in certain wave number regions (called bands) and does not absorb outside these bands. However, the amount of absorption within these bands is quite dependent on the pressure and temperature of the medium as well as the path length of radiation. Several models have been suggested to describe the phenomenon [9, 14], and of these methods, the one chosen in this report is the statistical model. The parameters appearing in this model have been obtained from spectroscopic determination of the band absorption characteristics by calculating a total emissivity and fitting these calculations to the known experimental values for the total emissivity. The difficulty in applying these values to the present calculation is that they were determined in a pressure region different from the region of interest. However, the existing data up to 1 atm [10] can be extrapolated to 3·22 atm by use of the statistical model. In Appendix A, the statistical model is applied to make the following approximation for the band absorption:

$$\int_{\omega_i-(\Delta\omega_i/2)}^{\omega_i+(\Delta\omega_i/2)}\kappa^*\rho^*B^*(T^*)\exp[-\tau_\omega(s^{*'}, s^*)]\,d\omega$$

$$\approx B_i^*(T^*)\exp[-\tau_i(s^{*'}, s^*)]\,\alpha_i^*(T^*) \qquad (11)$$

where $\alpha_i^*(T^*)$ is the integrated absorption coefficient for the i^{th} band, and

$$\tau_i(s^{*'}, s^*) = a\sqrt{(T_{\text{ave}})}\,f[\eta_i(s^{*'}, s^*)] \qquad (12)$$

$$\left.\begin{aligned}\frac{1}{T_{\text{ave}}} &\equiv \left[\frac{1}{s^* - s^{*'}}\int_{s^{*'}}^{s^*}\frac{ds^{*''}}{(T^{*''}/T_2^*)^{3/2}}\right]^{2/3}\\ \eta_i(s^{*'}, s^*) &\equiv \frac{a_i}{a}T_{\text{ave}}^{-2}(s^* - s^{*'})\\ \text{and}\quad f(\eta) &\equiv \eta\,e^{-\eta}[I_0(\eta) + I_1(\eta)]\end{aligned}\right\} \qquad (13)$$

Of particular interest is the average temperature used in the calculation. This was chosen because the absorption is inversely dependent on the three-halves power of the temperature. Since the absorption is to be calculated along the path, this average temperature is the natural one to use. This model includes the "strong band" model and the "weak band" model. It may be noted at this point that, over limited ranges of pressure and optical path length, the absorption may be represented as $(P^*\rho^*L)^n$ [14, 15], but since the variation of optical path is large and the pressure is rather high, such an approximation is not worthwhile in this case. For water vapor, the parameters a and a_i have been found experimentally [9, 10]. These data have been extrapolated to $T_2^* = 730°\text{R}$ and 3·22 atm according to Appendix A, and resulting values are given in Table 1.

Reduced equation and boundary conditions. Now, for the set of discrete bands, the α_i and B_i

Table 1. *Absorption coefficients for steam at* 730°R *and* 3·22 *atmospheres* [9]

i	a_i	ω_i (cm^{-1})	a
1	0·657	500	0·831
2	1·968	1587	↓
3	1·418	3704	
4	0·134	5348	
5	0·093	7246	
6	0·004	9091	

are made dimensionless by relating them to the maximum a_i and B_i, respectively. In defining

$$\beta_i \equiv \frac{a_i(T^*)}{a_{\max}(T_2^*)} \qquad h_i \equiv \frac{B_i^*(T^*)}{B_{\max}^*(T_2^*)}$$

$$H_i^{(1,2)}(T^*) = \frac{H_{w,i}^*(T^*)}{B_{\max}^*(T_2^*)} \tag{14}$$

the right-hand side of equation (10) can be written as

$$a_{\max}(T_2^*)\, B_{\max}^*(T_2^*)\, G(x^*, r^*, T^*)$$

where G is defined as

$$G = \sum_{i=1}^{N} \beta_i \Big\{ [H_i^{(1)}(T_1^*) - H_i^{(1)}(T^*)]\, f_i^{(1)} - [H_i^{(2)}(T^*) - H_i^{(2)}(T_2^*)]\, f_i^{(2)} + \frac{a_{\max}(T_2^*)}{\pi\, \Delta\omega_i} \int_{\Omega_s = 4\pi} \int_0^s \beta_i'[h_i(T^{*\prime}) - h_i(T^*)] \exp[-\tau_i(s^{*\prime}, s^*)]\, \mathrm{d}s'\, \mathrm{d}\Omega_s \Big\} \tag{15}$$

where $f_i^{(1)}$ and $f_i^{(2)}$ are the integrals in equation (10), and N is the number of bands constituting the spectrum. The function G is the non-dimensionalized net absorption of radiation at the point specified by co-ordinates (x^*, r^*). The turbulent diffusivity can also be nondimensionalized with respect to the maximum value; i.e. let e be defined as

$$e \equiv \frac{(k^*/\rho^* c_p^*) + \epsilon_h}{[(k^*/\rho^* c_p^*) + \epsilon_h]_{\max}} \tag{16}$$

and introduce

$$r \equiv \frac{r^*}{R_2^*} \qquad \Theta \equiv \frac{\ln T^* - \ln T_2^*}{\ln T_1^* - \ln T_2^*} \tag{17}$$

It can be shown [8] that $\partial P^*/\partial r^*$ is negligible, and if $\partial P^*/\partial x^*$ is assumed to be small, the equation of state becomes $\rho^* T^* = \rho_2^* T_2^*$. Using this equation of state and equations (16) and (17) gives equation (10) in the form

$$\frac{R_2^{*2}\, u_{\max}^*}{[(k^*/\rho^* c_p^*) + \epsilon_h]_{\max}}\, u \frac{\partial \Theta}{\partial x^*} - \frac{1}{r}\frac{\partial}{\partial r}\left(re\frac{\partial \Theta}{\partial r}\right) = \frac{R_2^{*2}\, a_{\max}\, B_{\max}^*}{\rho_2^* T_2^* c_p^* \ln(T_1^*/T_2^*)\, [(k^*/\rho^* c_p^*) + \epsilon_h]_{\max}} \tag{18}$$

A further non-dimensionalization may now be made by a scaling of the axial distance x^*; that is, introduce

$$\mathrm{d}z \equiv \frac{\mathrm{d}x^*}{R_2^*} \cdot \frac{[(k^*/\rho^* c_p^*) + \epsilon_h]_{\max}}{R_2^*\, u_{\max}^*} \tag{19}$$

But, since the maximum value of the eddy diffusivity will be much larger than the molecular diffusivity $k^*/\rho^* c_p^*$, z becomes

$$z = \int_0^{x^*} \frac{(\epsilon_h)_{\max}}{R_2^{*2}\, u_{\max}^*}\, \mathrm{d}x^* \tag{20}$$

Now, the remaining parameter on the right-hand side of equation (18) will be denoted by M, where

$$M = \frac{R_2^{*2} a_{\max}(T_2^*) B_{\max}^*(T_2^*)}{\rho_2^* T_2^* c_p^* \ln(T_1^*/T_2^*)\, (\epsilon_h)_{\max}} \tag{21}$$

This parameter represents the ratio of the absorption and emission of radiation to the turbulent diffusion of energy. Equation (18) may now be written as

$$u\frac{\partial \Theta}{\partial z} - \frac{1}{r}\frac{\partial}{\partial r}\left(re\frac{\partial \Theta}{\partial r}\right) = MG \tag{22}$$

The boundary condition at $z = 0$ is that the fluid temperature be uniform at a value of T_2^*, so that $\Theta(0, r) = 0$. At $r = R_1^*/R_2^* = \rho$, the temperature will be equal to T_1^*, and at $r = 1$ the temperature will be T_2^*, so that

$$\theta(z, \rho) = 1$$
$$\theta(z, 1) = 0$$

Method of solution

Since turbulent convection is quite likely to be the dominant mechanism of energy transfer in practical situations, it will be assumed that M is

small. This suggests that Θ be expanded in a power series about $M = 0$:

$$\Theta = \sum_{j=0}^{\infty} \Theta_j(z, r)\, M^j \tag{23}$$

Since G depends on the temperature, which, in turn, depends on M, G can be expanded in a Taylor series about $M = 0$:

$$G(x, r, \Theta) = G\,|_{M=0} + \left.\frac{\partial G}{\partial M}\right|_{M=0} M + \left.\frac{\partial^2 G}{\partial M^2}\right|_{M=0} \frac{M^2}{2} + \ldots \tag{24}$$

The substitution of these representations for Θ and G into equation (22) yields

$$\left[u\frac{\partial \Theta_0}{\partial z} - \frac{1}{r}\frac{\partial}{\partial r}\left(re\frac{\partial \Theta_0}{\partial r}\right)\right] + \left[u\frac{\partial \Theta_1}{\partial z} - \frac{1}{r}\frac{\partial}{\partial r}\left(re\frac{\partial \Theta_1}{\partial r}\right)\right] M + \left[u\frac{\partial \Theta_2}{\partial z} - \frac{1}{r}\frac{\partial}{\partial r}\left(re\frac{\partial \Theta_2}{\partial r}\right)\right] M^2 + \ldots = G(z, r, \Theta_0)\, M + \Theta_1 \frac{\partial G}{\partial \Theta}(x, r, \Theta_0)\, M^2 + \ldots \tag{25}$$

Since equation (25) must be valid for all M, the following sequence of boundary value problems can be formulated:

$$\left.\begin{aligned} u\frac{\partial \Theta_0}{\partial z} - \frac{1}{r}\frac{\partial}{\partial r}\left(re\frac{\partial \Theta_0}{\partial r}\right) &= 0 \\ \theta_0(0, r) = 0 \quad \Theta_0(z, \rho) &= 1 \quad \Theta_0(z, 1) = 0 \end{aligned}\right\} \tag{26}$$

and

$$\left.\begin{aligned} u\frac{\partial \Theta_1}{\partial z} - \frac{1}{r}\frac{\partial}{\partial r}\left(re\frac{\partial \Theta_1}{\partial r}\right) &= G(x, r, \Theta_0) \\ \Theta_1(0, r) = \Theta_1(z, \rho) &= \Theta(z, 1) = 0 \end{aligned}\right\} \tag{27}$$

and

$$\left.\begin{aligned} u\frac{\partial \Theta_j}{\partial z} - \frac{1}{r}\frac{\partial}{\partial r}\left(re\frac{\partial \Theta_j}{\partial r}\right) &= \frac{1}{(j-1)!}\left.\frac{\partial^{j-1} G}{\partial M^{j-1}}\right|_{M=0} \\ \Theta_j(0, r) = \Theta_j(z, \rho) &= \Theta_j(z, 1) = 0 \end{aligned}\right\} j = 2, 3, \ldots \tag{28}$$

These boundary value problems are linear with non-homogeneous (except for Θ_0) equations and homogeneous (except for Θ_0) boundary conditions.

The velocity profile $u(r)$ is known as a function of the radius, while the eddy diffusivity ϵ_h is a function of the velocity. Hence, when the eddy diffusivity dominates, e is dependent only on the velocity. However, near the boundaries, the eddy diffusivity vanishes so that the molecular diffusivity must be known in order to specify $e(r)$. However, the molecular diffusivity can be expressed in terms of the temperatures near the walls, which are the known boundary conditions for the problem. Hence, e is a function of the co-ordinates. At this point it will be assumed that e is a function only of the radius, that is, that the eddy diffusivity is independent of the axial co-ordinate even in the thermal entrance region. This assumption has been verified experimentally for flow tubes [6]. The consistency of this assumption can be determined by comparing the calculated temperature with the experimental temperature.

Solution for non-absorbing gas. The boundary value problem for Θ_0 is that associated with the development of the temperature profile in the thermal entrance region for a non-absorbing gas (as would be expected, since this is the physical significance of $M = 0$). This equation may be solved first by subtracting from Θ_0 the solution for the fully developed profile, Θ_{fd}, where

$$\Theta_{fd} = \frac{1}{C}\int_r^1 \frac{dr}{re(r)} \tag{29}$$

with

$$C = \int_\rho^1 \frac{dr}{re(r)} \tag{30}$$

Then, if $\Theta_{ent} = \Theta_0 - \Theta_{fd}$, equation (26) becomes

$$u\frac{\partial \Theta_{ent}}{\partial z} = \frac{1}{r}\frac{\partial}{\partial r}\left(re\frac{\partial \Theta_{ent}}{\partial r}\right)$$

with boundary conditions

$$\Theta_{ent}(0, r) = -(\Theta_{fd}); \quad \Theta_{ent}(z, \rho) = \Theta_{ent}(z, 1) = 0 \tag{31}$$

Now Θ_{ent} can be determined directly by the method of separation of variables; that is, represent Θ_{ent} as

$$\Theta_{ent} = \sum_{n=1}^{\infty} A_n \exp[-\lambda_n^2 z] R_n(r) \qquad (32)$$

where the pairs (R_n, λ_n) are the characteristic pairs defined by the following Sturm–Liouville problem:

$$\left.\begin{aligned} \frac{\mathrm{d}}{\mathrm{d}r}\left(re\frac{\mathrm{d}R_n}{\mathrm{d}r}\right) + ru\lambda_n^2 R_n = 0 \\ R_n(\rho) = R_n(1) = 0 \end{aligned}\right\} \qquad (33)$$

and the A_n are given by

$$A_n = \frac{-\int_{\rho}^{1} \Theta_{fd}\, urR_n\, \mathrm{d}r}{\int_{\rho}^{1} urR_n^2\, \mathrm{d}r} \qquad (34)$$

Hence, a solution has been obtained in terms of u and e. They have both been determined experimentally [8] for an annulus with radius ratio $\rho = 0{\cdot}2$ and are listed in Table 2. The

Table 2. Non-dimensional velocity profiles and eddy diffusivity for an annulus with radius ratio 0·2 at Reynolds numbers from 19 000 to 38 000

r	$u(r)$	$e(r)$	r	$u(r)$	$e(r)$
0·20	0	0·169	0·65	0·990	0·941
0·25	0·765	0·351	0·70	0·980	0·981
0·30	0·872	0·494	0·75	0·967	1·000
0·35	0·928	0·663	0·80	0·940	0·977
0·40	0·961	0·805	0·85	0·897	0·931
0·45	0·981	0·865	0·90	0·839	0·815
0·50	0·993	0·897	0·95	0·741	0·725
0·55	1·000	0·904	1·00	0	0·013
0·60	0·997	0·916			

method of determining u was by measurement using a Pitot-static tube. The values for e were obtained from the temperature profiles for the calibration runs (with dry air) at three different axial positions. From equation (26) it is clear that if u and Θ_0 are known experimentally for two values of z, then $e(r)$ can be deduced. Then, if Θ_0 is known at a third value of z, a second $e(r)$ can be determined and compared with the first. If these two determinations are the same then it is safe to assume that e is independent of z. However, because of the difficulty in differentiating experimental data, an alternative approach was taken. In this approach, an $e(r)$ is estimated (by differentiation), and then equation (33) is solved for the R_n with this value of $e(r)$ by means of Runge–Kutta numerical integration on an electronic computing machine. Since the R_n are determined up to an arbitrary multiplicative constant, the final requirement placed on the R_n is

$$\int_{\rho}^{1} ruR_n^2\, \mathrm{d}r = C$$

for the estimated $e(r)$. Now, the solution for Θ_0 is

$$\Theta_0 = \theta_{fd} + \sum_{n=1}^{\infty} A_n \exp[-\lambda_n^2 z] R_n(r) \qquad (35)$$

The Θ_0 given by equation (35) is determined by using the R_n corresponding to the initial estimate of $e(r)$ and is compared with the experimental values. Now, the estimated $e(r)$ is corrected until the calculated temperature agrees with the experimental values. This corrected $e(r)$ function is given in Table 2 for $\rho = 0{\cdot}2$ and corresponding value C is 4·964. The first seven R_n are listed in Table 3 and plotted in Fig. 1.

Shown in Fig. 2 is the solution to equation (35) for values of z from 0·05 to ∞ using the $e(r)$ in Table 1. Also shown in Fig. 2 are the experimental temperature profiles for a radius ratio of 0·2 at $z = 0{\cdot}1$, 0·135, and 0·170 and for a constant maximum velocity. The good agreement between the calculated values and the measured values at one z indicates that the correct e has been determined. The good agreement at three different values of z indicates that the value of $e(r)$ is independent of z (at least within the relatively small range of z for which experimental values were taken). This is in agreement with reference 6.

This same $e(r)$ function can now be used to calculate the temperature profile for different maximum velocities. The values of z corresponding to an experimental run for a fixed $u^*_{\max}$ can now be determined by comparing the profiles calculated by using equation (35) to the experimentally measured profiles. In this way it is possible to get a good correlation between

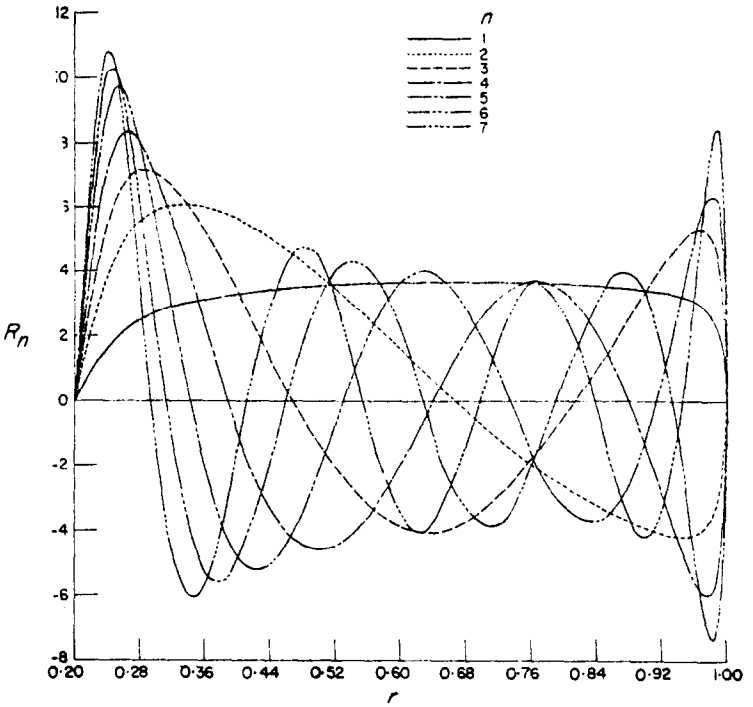

FIG. 1. First seven characteristic functions of equation (33).

Table 3. First seven characteristic functions defined by equation (33)

r	R_1	R_2	R_3	R_4	R_5	R_6	R_7
0·20	0	0	0	0	0	0	0
0·25	1·8004	4·2801	5·9977	7·7735	9·5699	10·2887	10·5752
0·30	2·7063	5·9130	6·9821	6·8755	5·2592	1·9968	−1·5575
0·35	3·0550	6·0316	5·6234	3·2213	−0·7648	−4·4255	−6·0266
0·40	3·2807	5·6324	3·4512	−0·6579	−4·5991	−5·0858	−2·1022
0·45	3·4407	4·8648	0·9665	−3·5313	−4·8445	−1·1140	3·5493
0·50	3·5512	3·8576	0·1293	−4·5841	−2·1385	3·1705	4·2480
0·55	3·6254	2·6855	−3·0091	−3·7933	1·4990	4·2362	0·0780
0·60	3·6671	1·4866	−3·9019	−1·7562	3·7900	1·7063	−3·6425
0·65	3·6825	0·4675	−4·0129	0·3526	3·9179	−1·4711	−3·5160
0·70	3·6784	−0·7246	−3·3874	2·5854	1·9247	−3·7597	0·2188
0·75	3·6507	−1·7856	−2·0940	3·6806	−1·1166	−2·6140	3·4544
0·80	3·6012	−2·6387	−0·4508	3·2966	−3·2906	0·7399	2·5027
0·85	3·5351	−3·2576	1·1681	1·8362	−3·6063	3·4022	−1·0187
0·90	3·4028	−3·8639	3·2778	−1·2364	−1·2184	3·3047	−4·1817
0·95	3·1316	−4·1416	5·0624	−4·9355	3·9705	−2·8408	1·1641
1·00	0	0	0	0	0	0	0

u^*_{max} and z for a wide range of z from a series of calibration runs [8]. Also, by using equation (35) in equation (6), it was found that x^*_{cr} corresponds to a value of z from equation (20) of 0·05. With $e(r)$ known and with z given by the maximum flow velocity, it is possible to estimate the effect of radiation by calculating Θ_1 and by comparing this calculated value with experimental measurements.

Solution for absorbing gas. In order to evaluate

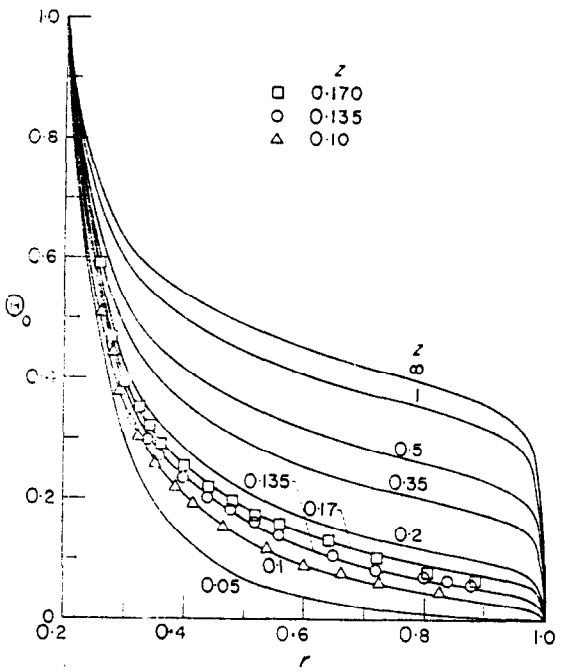

FIG. 2. Non-dimensional temperature profile for a non-absorbing gas.

Θ_1 it is necessary to evaluate $G(x, r, \Theta_0)$. This term can be evaluated when Θ_0 is known, but the numerical procedure is complicated. Because of this, two approximations were made in order to simplify the computation. These are:

(1) The gas to gas radiation was neglected for elements on lines of sight between the element under consideration and the inner wall. This is valid for the particular geometry considered (small inner radius), but would have to be checked again under other circumstances.

(2) In evaluating the absorption integrals $f_i^{(1)}, f_i^{(2)}, g_i^{(2)}$, the temperature was assumed to be given by $\Theta_0(x, r)$ and to be independent of x. As shown in Appendix B, this will give correct contributions for elements at axial stations close to x. While some error is introduced in evaluating the contributions from more distant axial stations, these contributions are small because most of the radiation is absorbed before reaching x.

In Appendix B, it is shown that G may be written as

$$G = \sum_{i=1}^{6} b_i \left(\frac{T_2^*}{T^*}\right) (\{H_i^{(1)}[\Theta_0(x, \rho)] - H_i^{(1)}[\Theta(x, r)]\} f_i^{(1)}(x, r) - \{H_i^{(2)}[\Theta(x, r)] - H_i^{(2)}[\Theta(x, 1)]\} f_i^{(2)}(x, r) - g_i^{(2)}(x, r)) \quad (36)$$

The number of bands N has been chosen as 6 for water vapor. The $f_i^{(1)}, f_i^{(2)}$, and $g_i^{(2)}$ are derived in Appendix B and can be evaluated by numerical integration. However, before numerical calculations for G can be made, it is necessary to determine the intensity of radiation at the surfaces.

Calculation of surface intensity. If the walls are black, then the surface intensity is determined by the temperature of the wall, but if the walls are not black, the reflected energy must be considered as part of the surface intensity. This may be accomplished by considering the following equations for a single band and a known temperature T^*:

$$H_i^{(1)} = \epsilon_1 h_i(\rho) + (1 - \epsilon_1) J_i^{(1)} \quad (37)$$

where $H_i^{(1)}$ is the intensity of surface one (the inner cylinder), and $J_i^{(1)}$ is the intensity impinging on surface one. Also,

$$H_i^{(2)} = \epsilon_2 h_i(1) + (1 - \epsilon_2) J_i^{(2)} \quad (38)$$

where $H_i^{(2)}$ is the intensity of surface two (the outer cylinder), and $J_i^{(2)}$ is the intensity impinging on surface two. The intensity impinging on surface one may be written as

$$J_i^{(1)} = F_i^{(2)} H_i^{(2)} + G_i^{(2)}(\rho) \quad (39)$$

where $F_i^{(2)}$ is the fraction of intensity from surface two that strikes surface one, and $G_i^{(2)}(\rho)$ is the intensity striking surface one as a result of the emission of the gas. Finally, the intensity impinging on surface two is

$$J_i^{(2)} = H_i^{(1)} F_i^{(1)} + G_i^{(1)}(1) + H_i^{(2)} F_i^{(s)} \quad (40)$$

where $F_i^{(1)}$ is the fraction of intensity $H_i^{(1)}$ that strikes surface two, $F_i^{(1)}$ is fraction of intensity $H_i^{(2)}$ that strikes surface two (itself), and $G_i^{(1)}(1)$ is the emission of the gas that strikes surface two. This gives four equations and four unknowns, which may be written as

$$\begin{pmatrix} 1 & 0 & -(1-\epsilon_1) & 0 \\ 0 & 1 & 0 & -(1-\epsilon_2) \\ 0 & -F_i^{(2)} & 1 & 0 \\ -F_i^{(1)} & -F_i^{(s)} & 0 & 1 \end{pmatrix} \begin{pmatrix} H_i^{(1)} \\ H_i^{(2)} \\ J_i^{(1)} \\ J_i^{(2)} \end{pmatrix} = \begin{pmatrix} \epsilon_1 h_i(\rho) \\ \epsilon_1 h_i(1) \\ G_i^{(2)}(1) \\ G_i^{(2)}(1) \end{pmatrix} \tag{41}$$

Taking the inverse of this matrix yields equation (42):

$$\frac{1}{\Delta_i} \begin{pmatrix} 1-(1-\epsilon_1)F_i^{(s)} & (1-\epsilon_1)F_i^{(2)} & (1-\epsilon_1)[1-(1-\epsilon_2)F_i^{(s)}] & (1-\epsilon_2)(1-\epsilon_2)F_i^{(2)} \\ (1-\epsilon_2)F_i^{(1)} & 1 & (1-\epsilon_1)(1-\epsilon_2)F_i^{(1)} & (1-\epsilon_2) \\ (1-\epsilon_2)F_i^{(1)}F_i^{(2)} & F_i^{(2)} & [1-(1-\epsilon_2)F_i^{(s)}] & (1-\epsilon_2)F_i^{(2)} \\ F_i^{(1)} & (1-\epsilon_1)F_i^{(1)}F_i^{(2)}+F_i^{(s)} & (1-\epsilon_1)F_i^{(1)} & 1 \end{pmatrix}$$

$$\times \begin{pmatrix} \epsilon_1 h_i(\rho) \\ \epsilon_2 h_i(1) \\ G_i^{(2)}(\rho) \\ G_i^{(1)}(1) \end{pmatrix} = \begin{pmatrix} H_i^{(1)} \\ H_i^{(2)} \\ J_i^{(1)} \\ J_i^{(2)} \end{pmatrix} \tag{42}$$

$$\Delta_i = 1-(1-\epsilon_2)[F_i^{(s)}+(1-\epsilon_1)F_i^{(1)}F_i^{(2)}]$$

By means of this equation the surface intensities are given in terms of the surface temperatures and emissivities and also in terms of the temperatures of the medium and its emission. It is now possible to evaluate G numerically for the pertinent conditions. The function G has been calculated for steam flowing in an annulus with radius ratio 0·2 and is plotted in Fig. 3 for $z = 0{\cdot}17$, at an inner wall temperature of 2000°R and a pressure 3·22 atm. The net absorption is negative near the inner wall—because the gas has been heated and is now emitting and is positive for the rest of the region.

Calculation of fluid temperature. The solution to the boundary value problem for Θ_1 may now be outlined, since $G(z, r, \Theta_0)$ has been determined (numerically for some special cases). Since the R_n have been defined, a solution utilizing them will be found. First, expand $G(z, r, \Theta_0)$ in a series of the characteristic functions R_n of the Sturm–Liouville problem as follows:

$$G(z, r, \Theta_0) = u(r) \sum_{n=1}^{\infty} \Phi_n(z)\, R_n(r) \tag{43}$$

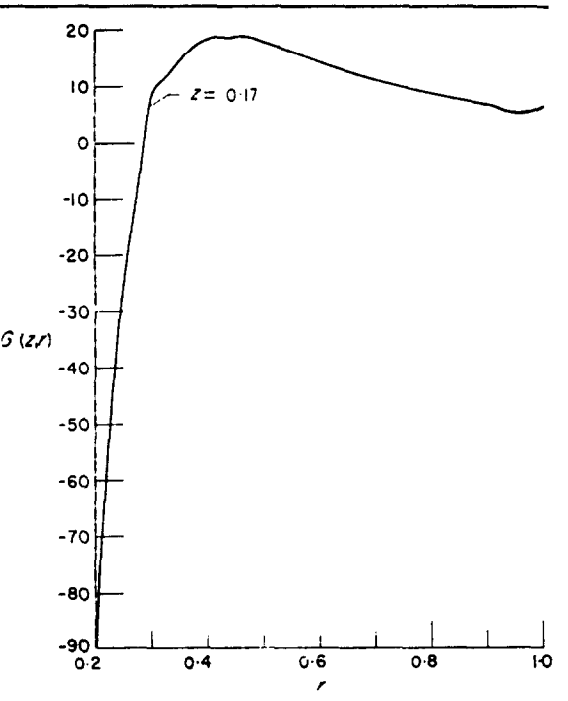

FIG. 3. Absorption of radiation for $T_1 = 2000$°R and $P = 3{\cdot}22$ atm.

It is a consequence of the theory of such expansions that

$$\Phi_n(z) = \frac{1}{C}\int_{\rho}^{1} G(z, r)\, R_n(r) r\, dr \qquad (44)$$

and are known functions of z (which is treated as a parameter in the expansion). Again using the Separation of Variables techniques Θ_1 is written as

$$\Theta_1(z, r) = \sum_{n=1}^{\infty} \chi_n(z)\, R_n(r) \qquad (45)$$

where the χ_n are to be determined from the differential equation. Notice that the boundary conditions on the inner and outer cylinders are satisfied directly. Equations (33), (44), and (45) may be substituted into equation (27), which becomes

$$\sum_{n=1}^{\infty}\left(\frac{d\chi_n}{dz} + \lambda_n\chi_n - \Phi_n\right) R_n = 0 \qquad (46)$$

with boundary condition $\chi_n(0) = 0$. Because the R_n are linearly independent, their coefficients must vanish, i.e.

$$\frac{d\chi_n}{dz} + \lambda_n^2\chi_n = \Phi_n \qquad (47)$$

Hence, the χ_n may be determined as

$$\chi_n(z) = \exp[-\lambda_n^2 z]\int_0^z \exp[\lambda_n^2\xi]\,\Phi_n(\xi)\, d\xi \qquad (48)$$

or, substituting for Φ_n

$$\chi_n = \frac{1}{C}\exp[-\lambda_n^2 z]\int_{\rho}^{1}\int_0^z R_n(r) \exp[\lambda_n^2\xi]\, G(\xi, r)\, d\xi r\, dr \qquad (49)$$

Thus, Θ_1 is specified in terms of G.

In order to calculate χ_n it is necessary to know G as a function of z from zero to the point of interest. However, G requires extensive calculation at each z. Consequently, an approximation for G is desirable in order to evaluate equation (49). Because the integrand in equation (49) is weighted more heavily for ξ near z, $G(\xi, r)$ can here be approximated by $G(z, r)$. With this approximation, the χ_n become

$$\chi_n(z) = \frac{1}{\lambda_n^2}(1 - \exp[-\lambda_n^2 z])\,\Phi_n(z) \qquad (50)$$

For conditions of $z = 0{\cdot}17$, $T_1^* = 2000°$R. and $P = 3{\cdot}22$ atm, the Φ_n are given in Table 4. The Θ_1 is found to be of the same order of magnitude as Θ_0, so that M must be small compared to 1 in order that equation (23) might be expected to converge.

This same procedure can be followed in obtaining the Θ_j for j greater than 1. An estimate of the magnitude of Θ_2 has been made for the case considered herein. It was found that the right-hand side of equation (27) was of the same order of magnitude as the right-hand side of equation (28) for Θ_2. Consequently, Θ_2 is the same order of magnitude as Θ_1, so that if M is small compared to 1, Θ_2 and higher terms can be neglected. For this situation

$$\Theta = \Theta_0 + M\Theta_1 \qquad (51)$$

Heat transferred to gas

The amount of energy transferred to the gas, as a result of both convection–conduction and radiation, may be calculated by multiplying the first term on the left-hand side of equation (7) by $2\pi r^*\, dr^*\, dx^*$ and integrating from R_1^* to R_2^* and from 0 to x^*. This yields

Table 4. Expansion coefficients and characteristic values

h	1	2	3	4	5	6	7
λ_n	1·5484	5·3654	8·8428	12·1094	15·4167	18·6832	21·8587
λ_n^2	2·3975	28·7877	78·1944	146·6376	237·674	349·157	477·804
$-A_n$	0·1256	0·0253	0·0135	0·0098	0·0080	0·0064	0·0053
B_n	0·8929	0·0037	0·0079	0·0001	0·0025	0·0003	0·0012
C_n	7·1077	0·1456	0·5864	0·0760	0·3165	0·0555	0·2223
D_n	0·0982	0·0046	0·0063	0·0015	−0·0001	−0·0005	−0·0004
Φ_n (0·17)	3·2925	0·5091	−0·6088	−1·2863	−1·0688	−1·2462	−0·9900

$$Q^* = 2\pi c_p^* \rho_2^* T_2^* u_{\max}^* R_2^{*2} \ln \frac{T_1^*}{T_2^*} q(z) \qquad (52)$$

where

$$q(z) = \int_\rho^1 ru\Theta(z, r)\, dr \qquad (53)$$

For a non-absorbing gas, this becomes

$$q(z) = \int_\rho^1 ru\Theta_0(z, r)\, dr = \int_\rho^1 ru\theta_{fd}\, dr + \sum_{n=1}^{\infty} A_n \exp[-\lambda_n^2 z] \int_\rho^1 ruR_n\, dr \qquad (54)$$

and if $\rho = 0{\cdot}2$

$$q(z) = 0{\cdot}18378 + \sum_{n=1}^{\infty} B_n \exp[-\lambda_n^2 z] \qquad (55)$$

where the B_n are given in Table 4. Hence, if Q_∞ is defined as

$$Q_\infty = 0{\cdot}18378 \ln \frac{T_1^*}{T_2^*} 2\pi c_p^* \rho_2^* T_2^* u_{\max}^* R_2^{*2} \qquad (56)$$

then for $\lambda_2^2 z \geqslant 5$ equations (55) and (56) may be substituted into equation (52) which becomes:

$$\frac{Q_{na}}{Q_\infty} \approx 1 - B_1 \exp[-\lambda_1^2 z]$$

For an absorbing gas,

$$q(z) = \int_\rho^1 ru(\Theta_0 + M\Theta_1)\, dr$$

which, for small M and $\lambda_2^2 z \geqslant 5$, can be substituted into equation (52) which becomes:

$$Q_{\text{abs}} = Q_{na} + 1{\cdot}09609 M D_1 C_1 Q_\infty \quad (\rho = 0{\cdot}2) \qquad (57)$$

where C_1 and D_1 are given in Table 4.

RESULTS AND DISCUSSION

The procedures developed in the preceding sections permit calculations of the effect of radiation on temperature profiles in channels for absorbing and non-absorbing gases. As an indication of the usefulness of the methods presented, analytical and experimental results are compared in Fig. 4 for the previously mentioned case of steam flowing in an annulus. The solid lines in Fig. 4 show temperature profiles that are calculated by using velocity profiles and eddy diffusivities determined from experiments with air. For a single run at 1·0 atm

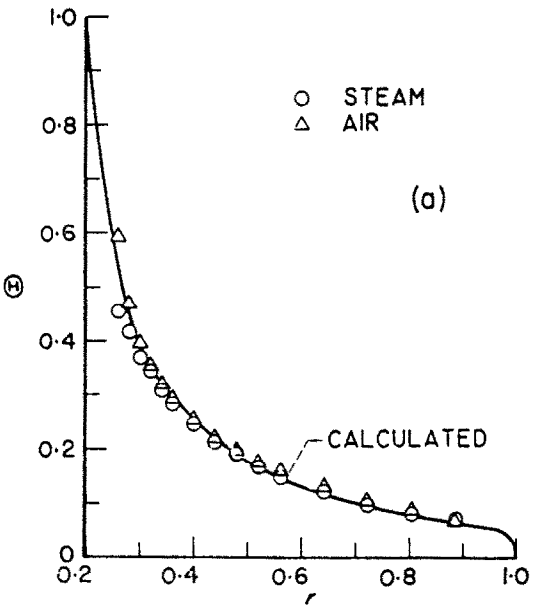

FIG. 4(a). Effect of radiation on temperature profile with $T_1 = 2000°R$.

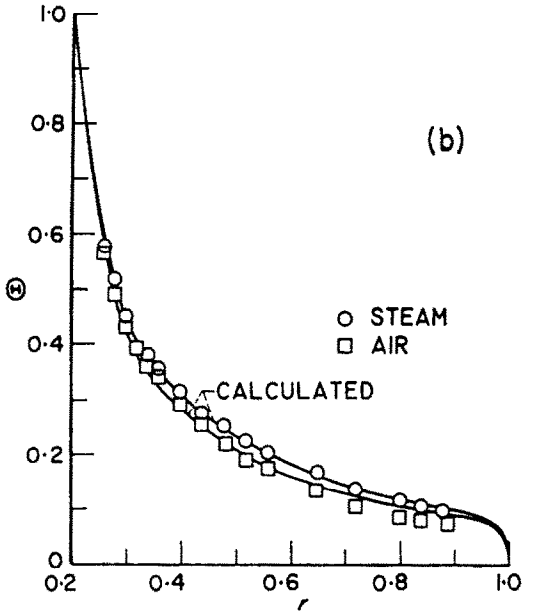

FIG. 4(b). Effect of radiation on temperature profile with $T_1 = 2000°R$.

the results may be seen in Fig. 4(a), and for a single run at 3·22 atm, where $M = 0{\cdot}034$, the results appear in Fig. 4(b). For the low pressure [Fig. 4(a)] no effect of absorption is observed. Both analytical and experimental data shown indicate agreement between air and low pressure steam. The effect of increasing the pressure, thereby increasing the opacity (and M) is to increase the temperature by a maximum of 7 per cent, and to increase the heat transferred by 4 per cent. The measured temperature difference between steam at 3·22 atm pressure and air is compared with the calculated difference in Fig. 5.

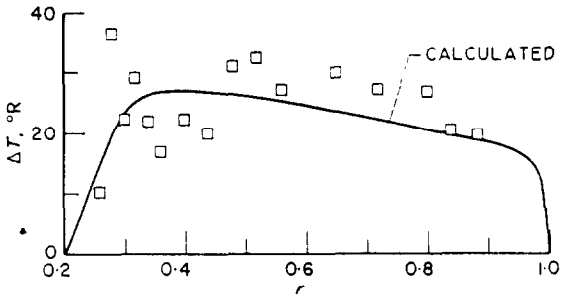

FIG. 5. Measured temperature difference between absorbing medium (steam at $T_1 = 2000°R$ and $P = 3{\cdot}22$ atm) and air.

The agreement is reasonable in light of a possible 10 degree error in determining the temperature difference. Unfortunately, no more experimental data were taken, so that a statistical error analysis could not be made.

For the steam conditions considered, the radiation effect will manifest itself as an increase in the temperature at any point because the absorption at that point increases faster with M than the emission. For comparable conditions, this result is in agreement with reference 4.

The heat transferred to the gas was calculated from the solutions for the temperature profile. The effect of radiation is to increase the heat transferred to the gas. For the conditions in the experiment the effect was only of the order of 4 per cent.

CONCLUDING REMARKS

A study has been made of the turbulent convection and thermal radiation absorption phenomena for a non-gray gas with variable density in the thermal entrance region of an annulus. The techniques developed for this special problem can be applied to more general problems as long as the radiation interaction parameter M is small. This parameter, which expresses the amount of radiation absorption compared to the turbulent convection, must remain small because the solution for an absorbing gas was obtained by perturbing the solution to the equivalent problem for a non-absorbing gas in powers of M.

In order to solve the thermal entrance problem for a non-absorbing gas both the velocity profile and the eddy diffusivity have to be known. For the particular analysis presented herein they were determined experimentally. For the interacting gas the absorption properties must be known. In this analysis they were obtained by adapting the experimental values for isothermal volumes for use in non-isothermal volumes by means of an appropriate average temperature. However, if the spectral data were not available, the medium could be considered a gray gas and solutions could be obtained in the same manner.

Analytical and experimental results were compared for the case of water vapor flowing at Reynolds numbers near 20 000 at a pressure of 3·22 atm with an inner wall temperature of 2000°R. The radius ratio for the annulus was 0·2. The temperature profile was measured at a point 15 diameters downstream of the start of the heated section. For these conditions, M is 0·034, and the requirements of the analysis are fulfilled. For these conditions, the temperature is increased by 7 per cent at the maximum, and the heat transferred is increased by 4 per cent due to absorption. The experimental measurements for the temperature profile and the heat transferred agree well with the calculated values.

REFERENCES

1. V. N. ADRIANOV and S. N. SHORIN, Radiant heat transfer in a flowing radiating medium. Translated from *Izv. Akad. Nauk., S.S.S.R., Otd. Tekh. Nauk.*, No. 5, 46–50 (1958). (From *AEC-TR*-3928).
2. E. A. SIDOROR, Connective and radiative heat-exchange in an absorbing medium. Translated from *Vaprocy Teploobmena*, p. 49 (1959). From Purdue Univ., Radiative Transfer Project Translation, *TT*-3 (June 1961).
3. A. N. RUMYNSKII, Boundary layer in radiating and

absorbing media, *J. Amer. Rocket Soc.* 32, 1135–1138 (1962).
4. R. Viskanta, Interaction of heat transfer by conduction, convection, and radiation in a radiating fluid. Paper 62-*WA*-189, ASME (1962).
5. R. G. Deissler and C. S. Eian, Analytical and experimental investigation of fully developed turbulent flow of air in a smooth tube with heat transfer with variable fluid properties. *NACA TN* 2629 (1952).
6. P. H. Albrecht and S. W. Churchill, The thermal entrance region in fully developed turbulent flow, *J. Amer. Inst. Chem. Engrs* 268–273 (1960).
7. E. Y. Leung, W. M. Kays and W. C. Reynolds, Heat transfer with turbulent flow in concentric and eccentric annuli with constant and variable heat flux. Rep. *AHT*-4, 109. Thermosciences Division, Department of Mechanical Engineering, Stanford University (1962).
8. Lester D. Nichols, Analytical and experimental determination of the fluid temperature profile in the entrance region of an annular passage considering the effect of convection and radiation. Ph.D. Thesis, Case Institute of Technology (1963).
9. S. S. Penner, *Quantitative Molecular Spectroscopy and Gas Emissivities*, pp. 320–327. Addison-Wesley, New York (1959).
10. D. Burch and D. Gryvnak, Infrared radiation emitted by hot gases and its transmission through synthetic atmospheres. Aeroneutronic Division, Publ. *U*-1929.
11. J. O. Hirschfelder, C. F. Curtiss and R. B. Bird, *Molecular Theory of Gases and Liquids*, pp. 720–728. John Wiley, New York (1954).
12. S. Chandrasekhar, *Radiative Transfer*, pp. 1–11. Clarendon Press, Oxford (1950).
13. V. Kourganoff, *Basic Methods in Transfer Problems*. Clarendon Press, Oxford (1952).
14. G. N. Plass, Useful representations for measurements of spectral band absorption, *J. Opt. Soc. Amer.* **50**, 868–875 (1960).
15. J. T. Bevans and R. V. Dunkle, Radiant interchange within an enclosure, Part I, *Trans. Amer. Soc. Mech. Engrs* **E81** 1–5 (1960).

APPENDIX A

Determination of Band Absorption

The representation of the band absorption by the water vapor will be determined by use of the statistical model; that is, the integral

$$\int_{\omega_i-(\Delta\omega_i/2)}^{\omega_i+(\Delta\omega_i/2)} \kappa_\omega^* \rho^* B_\omega(T^*) \exp\left[-\tau_\omega(s^{*\prime}, s^*)\right] \mathrm{d}\omega \tag{A1}$$

will be replaced by

$$K_i^* \rho^* B_{\omega_i}(T^*) \exp\left[-\tau_i(s^{*\prime}, s^*)\right] \Delta\omega_i$$

where the optical path length τ_i must be expressed in terms of the physical properties of water vapor as well as the physical distance. On the basis of the statistical model [9] the τ_i can be expressed as

$$\tau_i(s', s) = \left(\frac{2\pi b^*}{\delta^*}\right) f\left[\frac{\alpha_i^* R_2^* P^*}{\Delta\omega} \frac{\delta^*}{2\pi b^*} (s - s')\right] \tag{A2}$$

where

$$f(\eta) = \eta\, \mathrm{e}^{-\eta} \left[I_0(\eta) + I_1(\eta)\right]$$

This representation for the optical path is chosen such that for the "weak band" approximation [i.e. $f(\eta) \approx \eta$] that the τ_i will approach

$$\alpha_i^* R_2^* P^* (s - s')/\Delta\omega = K_i \rho^* R_2^* (s - s').$$

This is the definition of α^*, and is known experimentally. However, the temperature of the medium is not uniform, and an extension of the method will be made wherein an average temperature will be used. Since the $\kappa_\omega^* \rho^*$ is inversely proportional to the three halves power of temperature, the natural average temperature to use is the one that will yield the correct value for the average absorption, i.e.

$$\frac{1}{T_{\mathrm{ave}}^{3/2}} = \frac{1}{s^* - s^{*\prime}} \int_{s^{*\prime}}^{s^*} \left(\frac{1}{T^{3/2}}\right) \mathrm{d}s^{*\prime\prime} \tag{A3}$$

where

$$T = \frac{T^*}{T_2^*}$$

Now, the dependence of

$$a = \frac{2\pi b^*}{\delta^*} \quad \text{and} \quad a_i = \frac{\alpha_i^* R_2^* P^*}{\Delta\omega}$$

on temperature must be determined. For the collision-broadened bands, it can be shown [9] that

$$a(T^*, P^*) = a(T_2^*, P^*)\sqrt{(T_{\mathrm{ave}})} \tag{A4}$$

and

$$a_i(T^*, P^*) = a_i(T_2^*, P^*) T_{\mathrm{ave}}^{-3/2} \tag{A5}$$

so that

$$\tau_i(s', s) = a(T_2^*, P^*)\sqrt{(T_{\mathrm{ave}})} f \frac{a_i(T_2^*, P^*)}{a(T_2^*, P^*)} T_{\mathrm{ave}}^{-2}\, s(1 - \xi') \tag{A6}$$

where $\xi' = s'/s$. Hence, when the temperature distribution is given, then the absorption properties are known. This representation includes both the "weak band" approximation [$f(\eta) \approx \eta$] and the "strong band" approximation

$$[f(\eta) \approx \sqrt{[(2/\pi)\eta)}].$$

The method is versatile in the sense that an extrapolation to different pressures may be estimated on the basis of individual band absorption data [10]. On the basis of this extrapolation the dependence of the absorption band on pressure is given for water vapor as

$$a(T_2^*, P^*) = a(T_2^*, P_0^*)\left(\frac{P^*}{P_0^*}\right)^{0.838} \quad \text{(A7)}$$

and

$$a_i(T_2^*, P^*) = a_i(T_2^*, P_0^*)\left(\frac{P^*}{P_0^*}\right)^{0.185} \quad \text{(A8)}$$

where the reference pressure P_0^* is 1 atm. Now it is possible to determine the absorption quantities for water vapor at any temperature and pressure in terms of the absorption quantities at the reference conditions. For water vapor at 3·22 atm and 730°R these quantities are presented in Table 2.

APPENDIX B

Evaluation of Radiation Interaction Integrals

The function G as given in equation (15) must be written in terms of the variables used in the analysis, that is, (x, r, Θ). To do this, first, break the integral over the entire solid angle into two sections (Fig. 6), so that G becomes

$$G = G^{(1)} + G^{(2)}$$

where

$$G^{(1)} = 2\sum_{i=1}^{6}\frac{\beta_i}{\pi}\int_0^L\int_0^{\cos^{-1}(\rho'/r)} \{[h_i(T_1^*) - h_i(T^*)]\exp[-\tau^{(1)}](0, s) + a_i(T_2^*, P^*)\int_0^1 T(\xi_1')[h_i(T^{*\prime}) - h_i(T^*)]\exp[-\tau_i^{(1)}](s_1', s_1)\,d\xi'\}\frac{(r\cos\theta_1 - \rho)}{s_1^2}\,d\theta_1\,dx_1 \quad \text{(B1)}$$

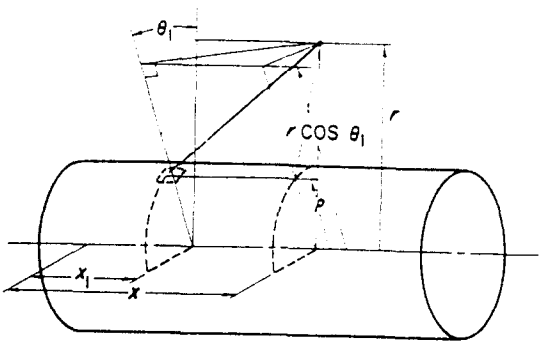

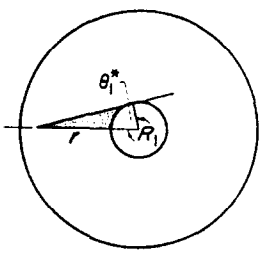

(a)

(a) From the inner cylinder to the gas.

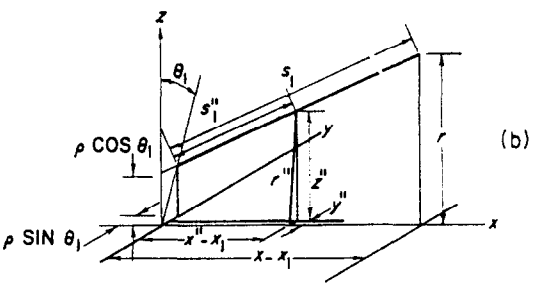

(b)

(b) Gas to gas radiation for shaded region in part (a).

FIG. 6. Co-ordinate sketches to determine radiation flux.

and

$$G^{(2)} = 2\sum_{i=1}^{6}\frac{\beta_i}{\pi}\int_0^L\int_0^{\theta_2^*} \{[h_i(T_2) - h_i(T_2^*)]\exp[-\tau_i^{(2)}](0, s_2) + a_i(T_2^*, P^*)\int T_{\text{ave}}[h_i(T^{*\prime}) - h_i(T^*)]\exp[-\tau_i^{(2)}(s_2', s_2)s_2]\,d\xi_2''\}\frac{(1 - r\cos\theta_2)}{s_2^2}\,d\theta_2\,dx_2 \quad \text{(B2)}$$

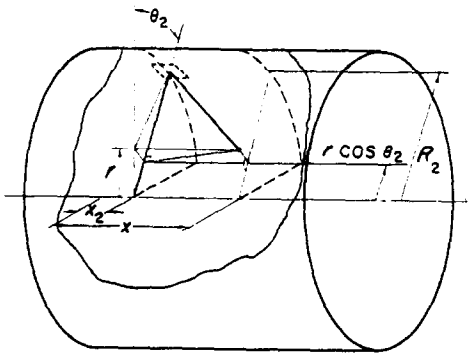

(c)

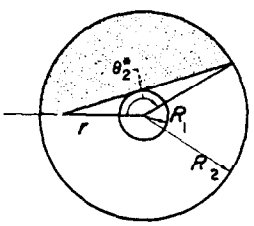

(c) From the outer cylinder to the gas.

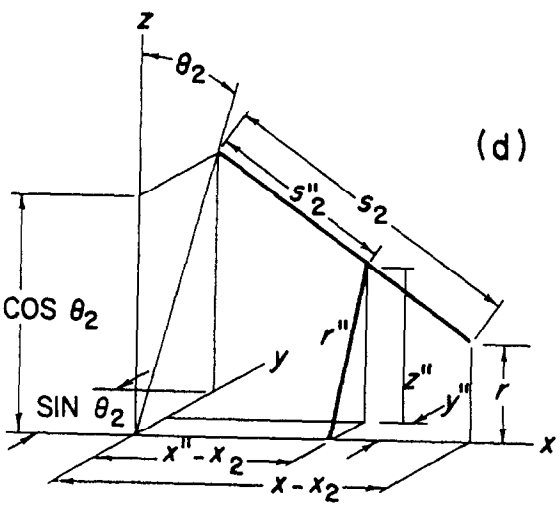

(d) Gas to gas radiation for shaded region in part (c).

FIG. 6. Co-ordinate sketches to determine radiation flux.

and the τ_i are given by equation (A6).

The $G^{(1)}$ and $G^{(2)}$ functions are greatly simplified if $a_i(T_2^*, P^*)$ is small. Then the gas to gas radiation can be neglected. However, in general, this is not the case, and these equations have to be used with no further simplification. But, for steam in the entrance region of an annulus, it can be shown that the gas to gas radiation is negligible in $G^{(1)}$. This is accomplished by evaluating the integral using the temperature profile given by Θ_0 and by comparing this term with the wall to gas term.

Another simplification can be made by considering the axial temperature variation of the temperature about a given x. It can be shown [8] that the integral over a line from a given point in the flow field to another point can be evaluated with small error by considering that the temperature profile at the first point be extended over the entire length of the flow region.

The functions $G^{(1)}$ and $G^{(2)}$ may now be evaluated once a temperature profile is specified. If the following integrals are defined

$$f_i^{(1)}(x, r) = \frac{\pi}{4} \int_0^5 \int_0^{\cos^{-1}\rho/r} \exp\left[-\tau_i(0, s_1)\right] \frac{\rho(r\cos\theta_1 - \rho)}{(y_1^2 + r^2 - 2r\rho\cos\theta_1 + \rho^2)^{3/2}} \, d\theta_1 \, dy_1 \quad \text{(B3)}$$

$$f_i^{(2)}(x, r) = \frac{\pi}{4} \int_0^5 \int_0^{\cos^{-1}\{\rho^2 - \sqrt{[(1-\rho^2)(r^2-\rho^2)]}/r\}} \exp\left[-\tau_i^{(2)}(0, s_2)\right] \frac{(1 - r\cos\theta_2)}{(y_2^2 + r^2 - 2r\rho\cos\theta_2 + \rho^2)^{3/2}} \, d\theta_2 \, dy_2 \quad \text{(B4)}$$

where $y_1 = x_1 - x$ and $y_2 = x_2 - x$, and

$$g_i^{(2)}(x, r) = \frac{4}{\pi} a_i \int_0^5 \int_0^{\cos^{-1}\{\rho^2\sqrt{[(1-\rho^2)(r^2-\rho^2)]}/r\}} \int_0^1 T(r') \{h_i[T^*(r)] - h_i(T^*(r'))\} \exp\left[-\tau_i^{(2)}(s_2', s_2)\right] d\xi_2' \frac{(1 - r\cos\theta_2)}{y_2^2 + r^2 - 2r\rho\cos\theta_2 + \rho^2} \, d\theta_2 \, dy_2 \quad \text{(B5)}$$

G can be written as shown in equation (36).

Numerical results for steam with $T_1^* = 2000°R$ and $P^* = 3{\cdot}22$ atm are presented in Figs. 7 to 9.

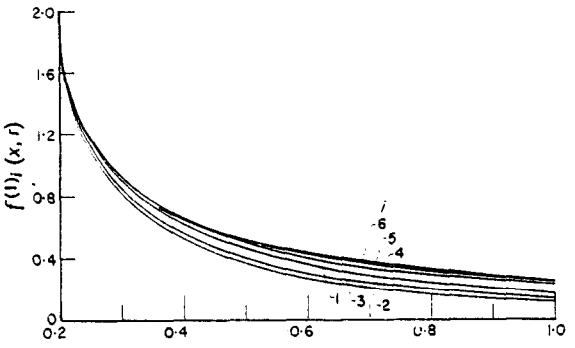

FIG. 7. Absorption integrals with $T_1 = 2000°R$ and $P = 3{\cdot}22$ atm.

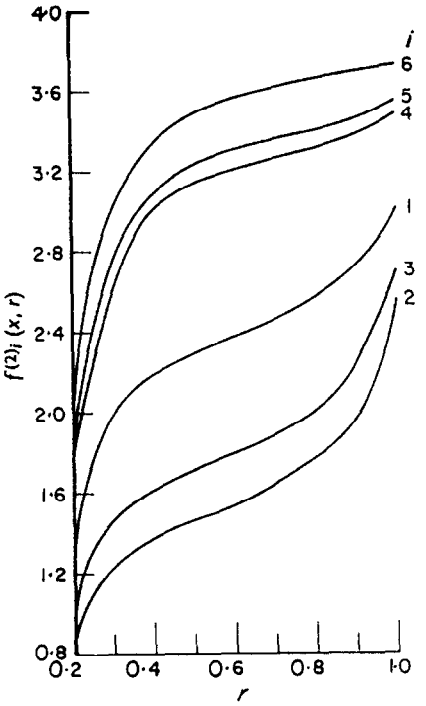

FIG. 8. Absorption integrals with $T_1 = 2000°R$ and $P = 3{\cdot}22$ atm.

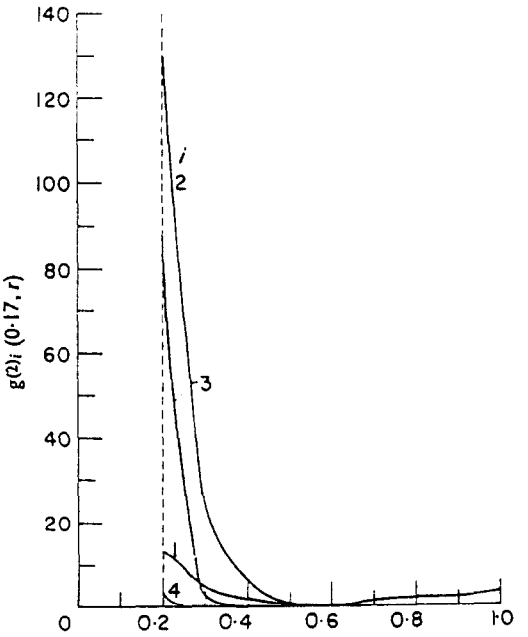

FIG. 9. Non-dimensional gas emission integrals defined in equation (B5) for $T_1 = 2000°R$ and $P = 3{\cdot}22$ atm.

APPENDIX C

Evaluation of Radiation Flux Integrals

The terms representing the intensity impinging on a surface may be obtained by an integration over the appropriate surface as follows:

$$F_i^{(1)} = \frac{4}{\pi}\int_0^5\int_0^{\cos^{-1}\rho} \exp\left[-\tau_i^{(2)}(0, s_2)\right] \frac{(1-\rho\cos\theta)(\cos\theta-\rho)}{(x^2+1-2\rho\cos\theta+\rho^2)^2}\,d\theta\,dx \tag{C1}$$

$$F_i^{(2)} = \frac{4}{\pi}\int_0^5\int_0^{\cos^{-1}\rho} \exp\left[-\tau_i^{(1)}(0, s_1)\right] \frac{(1-\rho\cos\theta)(\cos\theta-\rho)}{(x^2+1-2\rho\cos\theta+\rho^2)^2}\,\rho\,d\theta\,dx \tag{C2}$$

$$F_i^{(3)} = \frac{4}{\pi}\int_0^5\int_0^{\cos^{-1}(2\rho^2-1)} \exp\left[-\tau_i^{(2)}(0, s_2)\right] \frac{(1-\cos\theta)^2}{[x^2+2(1-\cos\theta)]^2} \tag{C3}$$

$$G_i^{(2)} = a_i\frac{4}{\pi}\int_0^5\int_0^{\cos^{-1}\rho}\int_0^1 T(r'')h(r'') \exp\left[-\tau_i^{(2)}(0, s'')\right] d\xi'' \times \frac{(1-\rho\cos\theta)(\cos\theta-\rho)\,d\theta\,dx}{(x^2+1-2\rho\cos\theta+\rho^2)^{3/2}} \tag{C4}$$

$$G_i^{(1)} = a_i \frac{4}{\pi} \int_0^5 \int_0^{\cos^{-1}(2\rho^4 - 1)} \int_0^1 T(r'')h_i(r'') \exp\left[-\tau_i^{(2)}(0, s'')\right] d\xi'' \times \frac{(1 - \cos\theta)^2 \, d\theta \, dx}{[x^2 + 2(1 - \cos\theta)]^{3/2}}$$

$$+ a_i \frac{4}{\pi} \int_0^5 \int_0^{\cos^{-1}\rho} \int_0^1 T(r'')h_i(r'') \exp\left[-\tau_i^{(1)}(0, s'')\right] d\xi'' \times \frac{(1 - \rho\cos\theta)(\cos\theta - \rho) \, d\theta \, dx}{(x^2 + 1 - 2\rho\cos\theta + \rho^2)^{3/2}} \quad \text{(C5)}$$

Résumé—L'influence de l'absorption de rayonnement sur le profil de température et le transport de chaleur dans un milieu absorbant s'écoulant dans un tuyau annulaire, a été examinée analytiquement.

Dans l'analyse, un écoulement turbulent d'un gaz non gris avec une densité variable et des coefficients d'absorption dépendant de la température est considéré. Les résultats de l'analyse sont comparés avec ceux d'une expérience effectuée avec de la vapeur d'eau s'écoulant à des nombres de Reynolds voisins de 20 000 à des pressions de 1 et 3,22 atm dans un tuyau annulaire avec un rapport de rayons de 0,2. Le résultat théorique est en accord avec le résultat expérimental que pour une température de la paroi intérieure de 1110°K et une pression de 3,22 atm, l'absorption du rayonnement augmente légèrement la température (environ de 7%). Ce résultat est également en accord qualitatif avec l'analyse de Viskanta pour un fluide au repos entre deux plaques parallèles.

Zusammenfassung—Der Einfluss der Strahlungsabsorption auf das Temperaturprofil und den Wärmeübergang an ein absorbierendes Medium, welches in einem Ringrohr strömt, wurde analytisch untersucht.

In der Analyse werden ein turbulenter, nicht-grauer Gasstrom mit variabler Dichte und temperaturabhängige Absorptionskoeffizienten berücksichtigt. Die Ergebnisse der Analyse werden mit denen eines Versuches verglichen, der mit Dampf durchgeführt wurde, welcher bei Reynoldszahlen nahe 20 000 bei Drucken von 1,0 vis 3,22 atm in einen Ringrohr vom Radienverhältnis 0,2 strömt. Das analytische Ergebnis stimmt mit dem Versuchsergebnis dahingehend überein, dass für eine Temperatur der Innenwand von 837°C und einem Druck von 3,22 atm die Strahlungsabsorption die Temperatur geringfügig erhöht (ungefähr 7%). Dieses Ergebnis steht auch in qualitativer Übereinstimmung mit den Ergebnissen der Analyse von Viskanta für eine stillstehende Flüssigkeit in einer planparallelen Geometrie.

Аннотация—В работе дано аналитическое исследование влияния поглощения излучения на профиль температур и перенос тепла к потоку поглощающей среды в канале. Анализировался турбулентиный прозрачный газовый поток с переменной плотностью и зависящими от температуры коэффициентами поглощения. Результаты анализа сравнивались с результатами экспериментального исследования течения жидкости в канале с соотношением радиусов 0,2 при числах Рейнольдса ~20 000 и давлениях 1,0 и 3,22 атм. Результат анализа согласуется с экспериментальным результатом: для внутренней температуры стенки в 2000°R и давлении в 3,22 атм поглощение излучения приводит к незначительному увеличению температуры (около 7%). Этот результат также качественно согласуется с результатами анализа Висканта для критического потока при плоскопараллельной геометрии.